

## Investigation of the bulk band structure of IV-VI compound semiconductors: PbSe and PbTe

V. Hinkel, H. Haak, C. Mariani,\* L. Sorba,<sup>†</sup> and K. Horn

*Fritz-Haber-Institut der Max-Planck-Gesellschaft, D-1000 Berlin 33, West Germany*

N. E. Christensen

*Max-Planck-Institut für Festkörperforschung, D-7000 Stuttgart 80, West Germany*

(Received 13 March 1989)

The bulk band structure of the IV-VI semiconductors PbSe and PbTe was determined experimentally through angle-resolved photoemission from cleaved PbSe(100) and PbTe(100) surfaces, using synchrotron radiation for photoexcitation. By analyzing spectra recorded in electron emission normal to the surface over a wide range of photon energies, it was found that a large number of photoemission peaks showed dispersion with photon energy, proving that the spectra can be interpreted through direct (i.e.,  $k$ -conserving) transitions. We analyze the dispersion in terms of transitions from occupied to unoccupied bands, on the basis of the free-electron final-state model. In order to relate the experimental data to calculated band structures, we have carried out linearized muffin-tin-orbital calculations for both solids. The experimental occupied band structure shows excellent agreement with these calculations. We discuss our results in the light of previous experimental and theoretical studies of these materials.

### I. INTRODUCTION

It is now widely recognized that the electronic structure of metals, semiconductors, and insulators can be determined by means of angle-resolved photoelectron spectroscopy. It has been shown that the bulk and surface emission can be separated, and that the bulk and surface band structure of a solid can be mapped in terms of an  $E(\mathbf{k})$  relation with high precision.<sup>1-5</sup> While a large range of metals has been investigated, including those in which relativistic effects, i.e., spin-orbit coupling, play an important role in shaping the bands, most studies of semiconductors have concentrated on those III-V compound semiconductors in which spin-orbit coupling, although important, does not dominate the band structure. Here, we treat the IV-VI compound semiconductors PbSe and PbTe, in which such effects are very pronounced. The band structure of these materials has been the subject of a number of calculations, which arrive at rather dissimilar results. As far as the interpretation of the photoelectron spectra are involved, Grandke *et al.*,<sup>6</sup> in one of the first extensive angle-resolved photoemission studies of semiconductor surfaces, concluded that photoemission spectra from the PbS, PbSe, and PbTe(100) surfaces could not be interpreted in terms of either direct transitions or nondirect transitions. They found reasonable agreement when analyzing their data using a "weighted-indirect-transition model," to be discussed below. Since the authors were restricted to two fixed photon energies from resonance lamps, their data base was necessarily limited as far as a variation of the wave vector normal to the surface  $\mathbf{k}_\perp$  is concerned. In view of the fact that in many angle-resolved photoemission data from well-ordered and not heavily reconstructed semiconductor surfaces a large

number of peaks can be interpreted in terms of direct transitions, we have reinvestigated these surfaces using synchrotron radiation for photoexcitation. We analyze our data in terms of the simple free-electron final-state model. This is a good first approximation since we can infer, directly from the data, those photon energies at which we reach either the center or the boundary of the Brillouin zone, and these values are in excellent agreement with those expected from a free-electron parabola. In order to provide a firm basis for the comparison of our data with calculations, we present new linearized muffin-tin-orbital (LMTO) calculations<sup>7,8</sup> for the band structure of these materials. We find very good agreement between the experimental data and the calculations, despite the fact that no corrections are taken into account in the comparison.

### II. EXPERIMENT

Photoemission experiments were carried out at the BESSY (Berliner Elektronen-Speicherring-Gesellschaft für Synchrotronstrahlung) storage ring, on the TGM 2 toroidal-grating monochromator,<sup>9</sup> giving us access to photon energies  $\hbar\omega$  from 9 to 200 eV. Spectra were recorded with a commercial angle-resolving photoelectron spectrometer (ADES 400 by VG Scientific Ltd., Great Britain), with a base pressure of  $1 \times 10^{-10}$  mbar. The joint resolution ranged from about 100 meV at  $\hbar\omega = 10$  eV to about 400 meV at 140 eV. The crystals were cleaved *in situ* by the double-wedge technique, and showed no sign of contamination even after measuring times of 10 h. The cleaved faces exhibited large terraces of flat surfaces, separated by a few large-scale steps. They showed excellent crystalline order as evidenced by a

sharp low-energy electron diffraction (LEED) pattern which was observed *in situ*, with no signs of twinning.

### III. DETAILS OF THE CALCULATION

The electronic structures of PbSe and PbTe were derived by means of the LMTO method<sup>7</sup> using a Dirac relativistic version.<sup>8</sup> The crystal structure is *B1* (rocksalt), and since this is a rather open structure we have optimized the LMTO scheme by introducing two (equivalent) "empty spheres." These are treated in the same way as usual atomic spheres in the self-consistency cycle, i.e., like atoms with no nuclear charge. The band structures were taken to be the unmodified eigenvalues obtained from the density-functional scheme within the local-density approximation (LDA). We used the exchange-correlation parametrization as given by von Barth and Hedin.<sup>10</sup> Experience from a large number of (zincblende-type) semiconductors has shown that this type of calculation yields accurate relative positions of the valence bands, whereas substantial errors in the energetic position of the conduction bands with respect to the valence bands (the "LDA band-gap problem") as well as the conduction-band dispersion are to be expected.<sup>11</sup> The analysis presented in the present work only needs the valence bands, and therefore the simple LDA band structures were assumed to represent a useful theoretical basis.

### IV. RESULTS AND DISCUSSION

The most common method for bulk band-structure determinations through angle-resolved photoemission is to take spectra along a high-symmetry direction of the crystal. The most practical solution for a crystal specimen with a low-index surface orientation involves the recording of spectra in normal emission. The lead chalcogenide semiconductors crystallize in the rocksalt structure, and the (100) surface is the cleavage face. Hence, when recording normal-emission spectra, we detect electrons with their wave vector lying along the  $\Gamma$ -*X* direction in the three-dimensional Brillouin zone. Such spectra, recorded with photon energies from 13 to 30 eV, are shown for PbSe(100) in Fig. 1. The spectra exhibit rich structure in the region from  $E_F$  to about 8 eV below  $E_F$ . It is quite obvious from Fig. 1 that some peaks exhibit large dispersion effects, i.e., shifts with photon energy; these have been connected by dashed lines for clarity. At the lowest photon energies, only the electron levels most closely situated with respect to  $E_F$  can be excited. As the photon energy increases, the deeper levels can also contribute. This effect is demonstrated in the spectra of Fig. 2. Some peaks, which are marked by asterisks, are due to excitation of the Pb *5d* level by second-order light from the monochromator grating. The lowest band (binding energy about 12 eV) is only observed for photon energies above 28 eV. The full range of peaks throughout the valence-band region is shown in the spectra in Fig. 2, which were recorded using photon energies from 35 to 140 eV. Here also, dispersion effects are quite obvious, particularly in the bands at 8 and 12 eV binding energy. The behavior of the peak at 8 eV binding energy is some-

what more complex, because here two peaks are superimposed, with the one at higher binding energy being stationary, while the one at lower binding energy disperses; this is particularly evident in the spectra recorded with photon energies between 40 and 65 eV. The coexistence of stationary and dispersing peaks from one particular band is direct evidence for the occurrence of direct *and* indirect transitions. Dispersion effects are also quite obvious in the region near the top of the valence bands. An analysis of the peaks in terms of the direct transitions will be presented below.

The close similarity of the physical properties of PbSe and PbTe should be reflected in their electronic structures and therefore in the photoemission spectra. This is in fact the case, as can be seen from a comparison of the PbSe(100) spectra in Figs. 1 and 2, and those of PbTe(100) shown in Figs. 3 and 4. Figure 3 shows the valence-band spectra of PbTe(100) recorded with photon energies from 9.5 to 30 eV. Here also, shifts of peaks with photon energies are evident, with one peak shifting from close to the valence-band maximum (VBM) to about 4 eV below the VBM. This peak is quite intense in this range of photon energies, and its behavior presents a text-

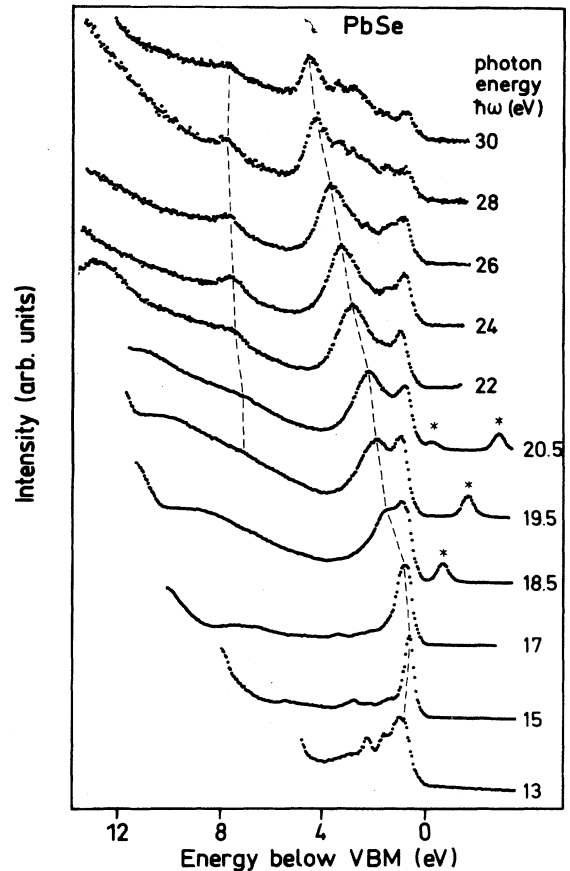


FIG. 1. Photoelectron spectra of the valence-band region of PbSe(100), recorded in normal emission; photon energies in the range from 13 to 30 eV as indicated in the figure.

book example of the manifestation of direct transition in angle-resolved photoelectron spectra. Often, considerable intensity variations occur in one particular peak as the photon energy is varied, such that dispersion effects are not immediately obvious, and only emerge from an analysis in which the energy of all peaks is plotted versus photon energy. Figure 3 provides a nice example in which dispersion can be seen immediately. The spectra recorded with higher photon energy (Fig. 4) also exhibit the same overall features as those of PbSe. The peak at about 8 eV binding energy is composed of two components, one of which is stationary, while the other disperses. Components from higher-order light are marked by asterisks as usual. No evidence for surface states was found in these normal-emission spectra.

In order to analyze the peaks in the spectra in terms of direct transitions, and to extract information about the occupied bands, one has to make assumptions about the

final-state bands. This is in fact the weak point of the band-mapping procedure, since calculations involving a realistic description of the final state, e.g., by using a time-reversed LEED final state, are usually not available. However, one can obtain an estimate of the shape of the final bands experimentally from the trend in peak shift with photon energy. This can be carried out in the so-called "structure plot," where the binding energy of all peaks with respect to the valence-band maximum is plotted over final energy. Now we use the fact that the band energies exhibit extrema at the Brillouin-zone center and boundaries, if the latter are true critical points<sup>12</sup> and therefore all peaks in the valence-band spectrum need to have their largest or smallest binding energy there. Consider the structure plot for the peaks in the PbTe spectra shown in Fig. 5. The band at around 6–8 eV binding energy is particularly instructive. Its binding energy exhibits a minimum close to  $E_{\text{final}} = 10$  eV ( $E_{\text{final}}$  with respect

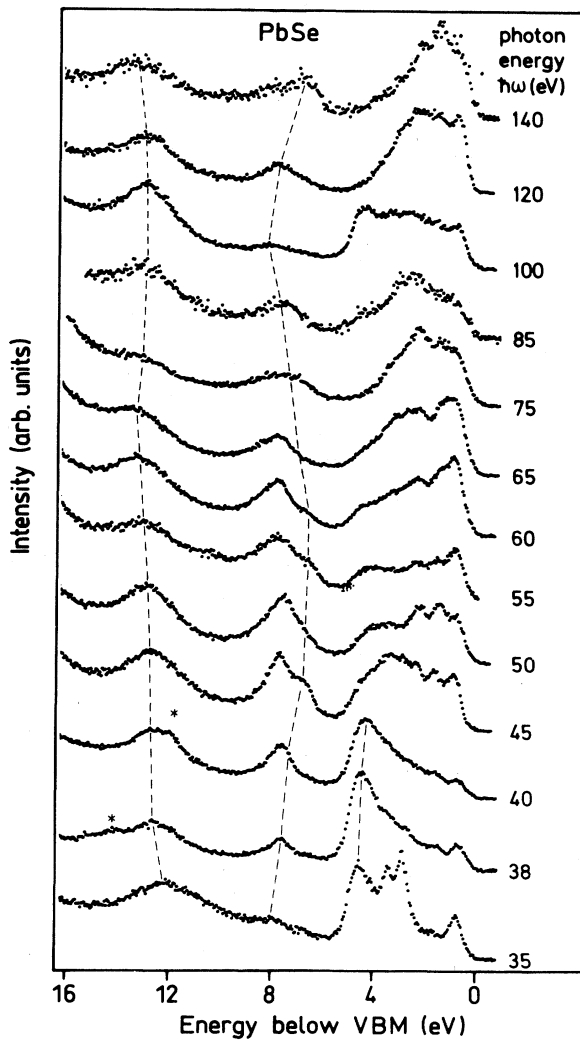


FIG. 2. Photoelectron spectra of the valence-band region of PbSe(100), recorded in normal emission over a photon-energy range from 35 to 140 eV.

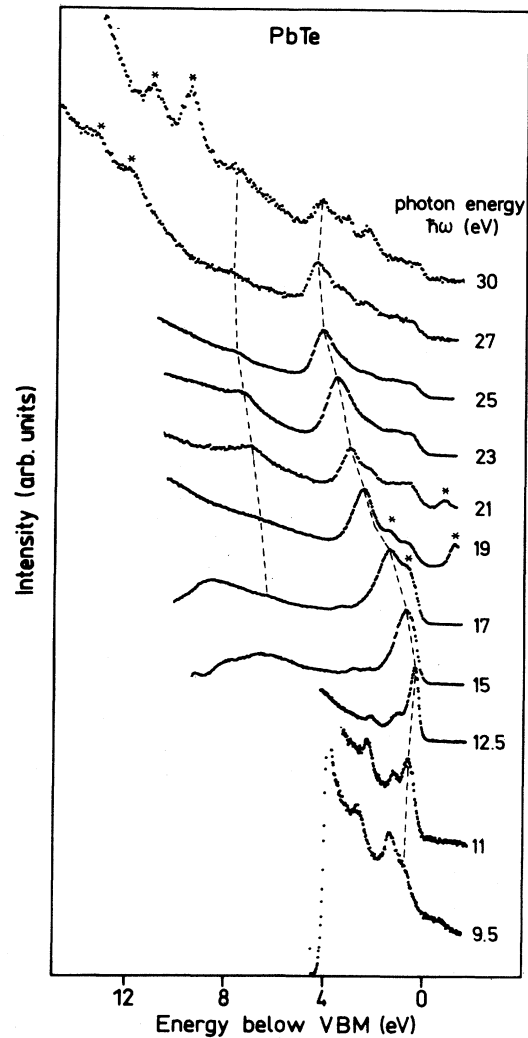


FIG. 3. Photoelectron spectra of the valence-band region of PbTe(100), recorded in normal emission; photon energies in the range from 9.5 to 30 eV as indicated in the figure.

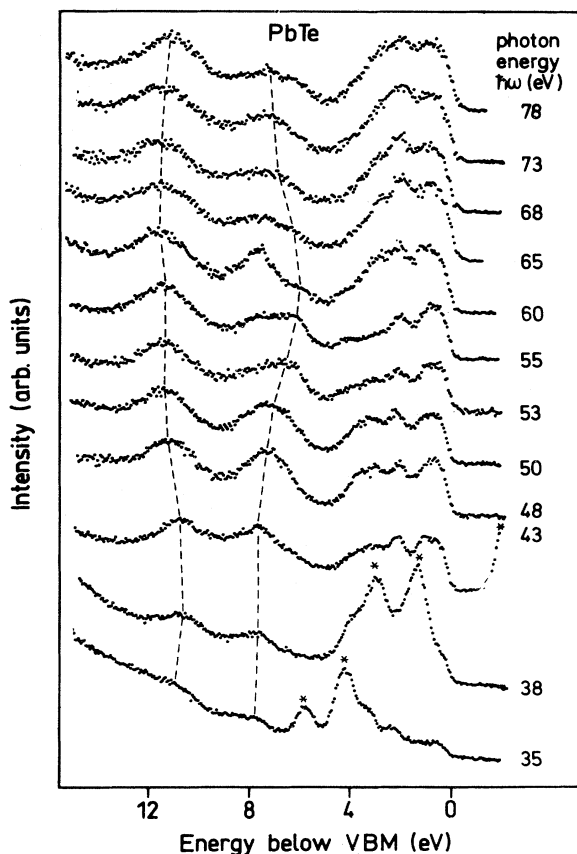


FIG. 4. Photoelectron spectra of the valence-band region of PbSe(100), recorded in normal emission over a photon-energy range from 35 to 78 eV.

to the Fermi energy  $E_F$ ), a maximum at 26 eV, and a further minimum at 53 eV. By recourse to calculated bands we know that this particular band has a binding-energy minimum at the  $\Gamma$  point and a maximum at the  $X$  point. Thus we can locate those photon energies at which direct transitions will take place at these points in  $k$  space; the

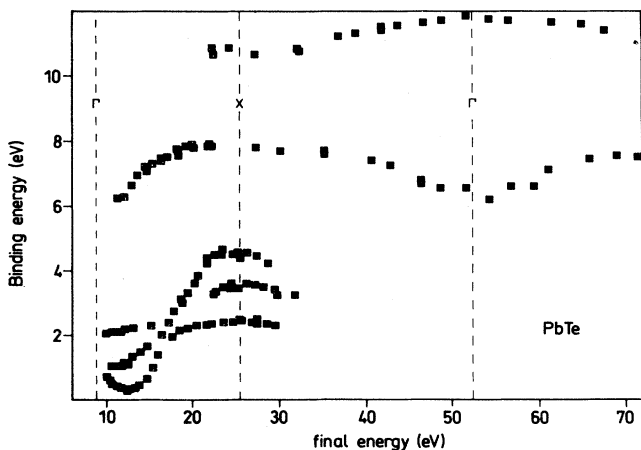


FIG. 5. Plot of binding energy of peaks in the spectrum of PbTe(100) vs electron kinetic energies.

$\Gamma$  point will be reached at photon energies where the electron final energy is 10 and 53 eV.

From the separation of the final energies at which the  $\Gamma$  and  $X$  points are reached, we can construct a rough shape of the final band, if we assume that it is described by a parabola with

$$E_{\text{final}} = \frac{\hbar^2 k^2 \alpha}{2} - V_0, \quad (1)$$

where  $V_0$ , the inner potential, is a free parameter, and  $\alpha=1.0$  for a free-electron parabola. By calculation the values for  $k$  for each of those transitions which occur at  $\Gamma$  or  $X$ , we obtain a best fit for the extrema shown in the structure plot of Fig. 5 for  $V_0=7.17$  eV. Based on this

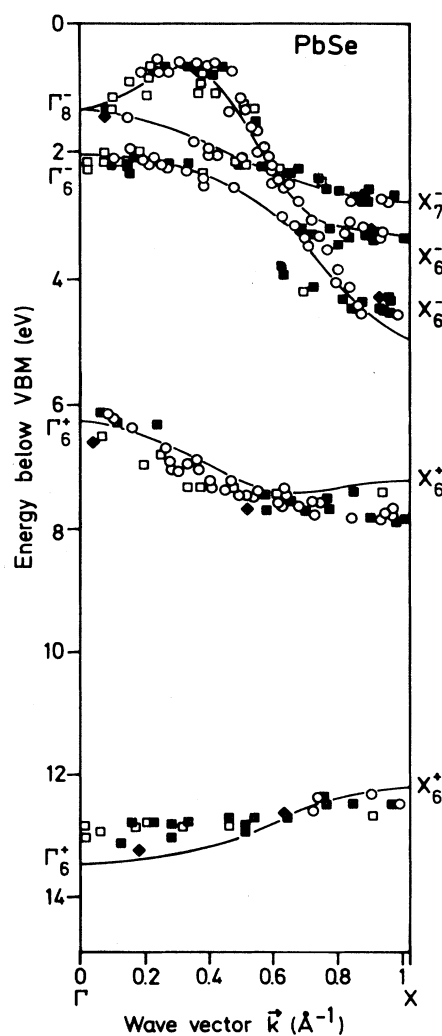


FIG. 6. Experimental band structure for PbSe, derived from spectra in Figs. 1 and 2. Transitions into the second, third, fourth, fifth, and sixth Brillouin zones are marked by triangles, open circles, solid squares, open squares, and solid diamonds. The lines represent the results of our LMTO band-structure calculation. [Energies are given relative to the valence-band maximum (VBM) at the  $L$  point.]

TABLE I. Experimental results for the critical-point energies of PbSe along the  $\Gamma$ - $X$  line, compared with the experimental determination of Grandke *et al.* (Ref. 6) and results from several band-structure calculations.

	Experiment		Calculations			
	This work	Grandke <i>et al.</i> <sup>a</sup>	APW <sup>b</sup>	EPM <sup>c</sup>	EPM <sup>d</sup>	LMTO <sup>e</sup>
$\Gamma_8^-$	1.45	1.8	1.83	2.0	1.8	1.35
$\Gamma_6^-$	2.2	2.5	2.43	2.6	2.35	2.05
$\Gamma_6^+$	6.25			5.75	5.15	6.25
$\Gamma_6^+$	12.95			24.55	14.95	13.45
$X_7^-$	2.75	3.2	2.99	3.2	3.85	2.75
$X_6^-$	3.3	3.7	3.43	3.6	4.2	3.3
$X_6^-$	4.45	5.1	4.94	4.9	6.4	4.95
$X_6^+$	7.7			5.65	6.8	7.2
$X_6^+$	12.35			24.30	13.30	12.2
spin-orbit splitting at $\Gamma$	0.75	0.6	0.60	0.55	0.55	0.7
spin-orbit splitting at $X$	0.55	0.5	0.44	0.35	0.35	0.55
$\Delta_6(\text{max})$	0.60	1.1	1.39	1.15	0.80	0.65

<sup>a</sup>Reference 6.

<sup>b</sup>In Ref. 6.

<sup>c</sup>Reference 18.

<sup>d</sup>Reference 13.

<sup>e</sup>This work.

value, we find that transitions take place at the  $X$  point at a kinetic energy of 26 eV, and at the  $\Gamma$  point at 8 and 52 eV. Thus there is good agreement between the experimental critical points and the values derived from the free-electron final band, giving confidence to our attempt to use this final band also for a determination of the shape of the occupied bands in the  $k$ -space between the Brillouin-zone center and boundary. A similarly good description for the final band was found in the structure plot also for PbSe, giving final energies of 9.5 eV ( $\Gamma$ ), 29.5 eV ( $X$ ), 58 eV ( $\Gamma$ ), and 94 eV ( $\Gamma$ ) at which the critical points were reached, with  $\alpha=1$ .

We have analyzed the dispersing peaks in the PbSe and PbTe spectra in terms of transitions from the occupied bands to this final band. The resulting experimental band structure of PbSe between  $\Gamma$  and  $X$  is shown in Fig. 6. For this plot, the inner potential  $V_0$  was derived from a structure plot similar to that shown for PbTe in Fig. 5. The best fit for  $V_0$  was 8.0 eV, close to the value for PbTe. The different symbols in the band structure mark direct transitions which take place in the second, third, higher (up to sixth) Brillouin zones. The two lowest bands are well characterized throughout the whole range of  $k$  between  $\Gamma$  and  $X$ . For the region closer to the VBM, three bands can be clearly identified at the  $X$  point. Around halfway through the Brillouin zone, band crossing renders an assignment difficult. However, two bands are well separated at  $\Gamma$ . Even for the most strongly dispersing bands, the data points from all transitions in the higher zones are quite close in  $E$  and  $k$ , indicating that our simple final state works well beyond all expectations. We shall attempt an explanation for the astonishing success of this simple ansatz below.

Also shown in Fig. 6 is the calculated LMTO band structure. The experimental bands have been lined up with respect to the valence-band maximum by taking the usual extrapolation to zero intensity in the spectra as the position of the VBM; the minimum binding energy of the experimental band is then 0.4 eV below the VBM. The energies of the critical points as derived from the present experiments, as well as the study of Grandke *et al.*<sup>6</sup> and several band-structure calculations<sup>6,13,14</sup> are given in Table I. The empirical-pseudopotential-method (EPM) bands deviate strongly from our experimental  $E(k)$  relations, particularly with respect to the position of the bands close to the VBM at the  $X$  point, but also as far as the total bandwidth is concerned. Consider the third band from the VBM: while its experimental bandwidth is about 2.2 eV, the value calculated by Martinez *et al.* is 3.9 eV. The energy of the third band from VBM at the  $X$  point also differs from the experimental value by almost 2 eV; larger discrepancies exist for the lowest band. In view of the way in which the parameters for the EPM calculation are derived, the discrepancy for the bands at higher binding energy is not surprising.

The bands calculated here by the LMTO method contain no adjustable parameters. For PbSe, one observes immediately that agreement between theory and experiment is very good for all bands. For the group of bands close to the VBM, the experimental data points lie on the calculated bands or not further than  $0.1 \text{ \AA}^{-1}$  and 0.2 eV away. The difference in energy between the topmost  $\Delta_6$  band and the VBM in the calculated band structure is about 0.9 eV, i.e., within 0.1 eV of the experimental value. In view of the difficulties in the precise experimental determination of the valence-band maximum, this

agreement is excellent. This statement also applies to the determination of the  $\Delta_6(\text{max})$  point, for which experimental and theoretical data are also given in Table I. Agreement is also very good for the two lower  $\Delta_6$  bands. In principle, deviations from experimental values are expected for these low-lying chalcogen *s*-derived bands because of shortcomings in the description within the local-density approximation. Jackson and Allen,<sup>15</sup> in their study of the occupied and unoccupied band structure of Si, Ge, GaAs, and ZnSe by x-ray photoelectron and bremsstrahlung isochromat spectroscopy and density-functional band-structure calculations, found that the calculated densities of state for the valence bands had to be shifted between 0.3 and 0.8 eV towards higher binding energies in order to obtain good agreement with each other. The amount of shift was determined by the character of the specific level and its degree of localization. The deviations were attributed by Jackson and Allen to self-energy corrections, which would have to be included in these calculations. Such self-energy corrections are well known, and are particularly strong in the nearly-free-electron metals, where deviations of up to 30% in the bandwidth occur.<sup>16</sup> In contrast to this, the present data suggest that any corrections to the present calculations cannot be simply given by a rigid shift to the bands, and that they would have to change sign between the lowest and second band. In view of the good overall agreement between the experimental and calculated bands, despite the strong localization (as derived from the amount of dispersion) of the two lowest bands, a straightforward conclusion about self-energy corrections such as that suggested by Jackson and Allen cannot be drawn from the present study.

In this context, PbSe is not an exception, because the same conclusions can be drawn from a comparison of the experimental band structure with the calculated bands of PbTe, shown in Fig. 7. The band structure shows quite similar features, with the band maximum of the highest  $\Delta_6$  band about  $0.2\text{--}0.3 \text{ \AA}^{-1}$  away from  $\Gamma$ ; as in PbSe, the valence-band maximum is located at the *L* point. The solid lines give the LMTO bands. For the *s*-derived  $\Delta_6$  bands at about 6–7 eV and 11.5–12.5 eV binding energy, the LMTO bands agree well with the experimental data, with respect to both binding energy and dispersion, although there seems to be an apparent splitting of the  $\Delta_6$  and  $\Delta_7$  bands at  $\Gamma$ , giving rise to a deviation between experimental and theoretical values of about 0.4 eV at this point. There seems to be a rigid shift in the  $\Delta_6$  band at a binding energy of around 6 eV when compared with theory; its dispersion is quite similar to the LMTO calculation. Energies of critical points for PbTe are collected, and are compared with results from other calculations in Table II. As far as the self-energy corrections are concerned, Fig. 7 shows that in the case of PbTe, the correction would have to change sign between the  $\Delta_6$  band at about 6 eV and that at about 12 eV binding energy. Such reversal of sign is not likely to be explained by the difference in localization and character of the band. This observation also excludes the possibility of interpreting our detailed *k*-dependent band-structure data in terms of a *k*-dependent self-energy correction.

The magnitude of spin-orbit interaction in the lead salts is one of the causes for the difficulties which are encountered in band-structure calculations; hence it is of interest to determine the spin-orbit splitting at specific points in the Brillouin zone. The spin-orbit splittings consist of contributions from the Se 4*p* and Te 5*p* levels (0.42 and 0.84 eV, respectively<sup>17</sup>) and the Pb 6*p* level [1.27 eV (Ref. 17)]. Depending on the character of the electron wave functions at specific points in the Brillouin zone, the spin-orbit splitting is expected to change.<sup>6</sup> From the dispersion of the experimental bands shown in Figs. 6 and 7, we have determined the spin-orbit splitting at the  $\Gamma$  and *X* points, i.e., the splitting between  $\Gamma_8^-$  and  $\Gamma_6^-$  and  $X_7^-$  and  $X_6^-$ . A comparison of the values given in Tables I and II shows that the agreement between the experimentally determined values and the LMTO calculations is very good for PbSe, whereas for PbTe there is a some-

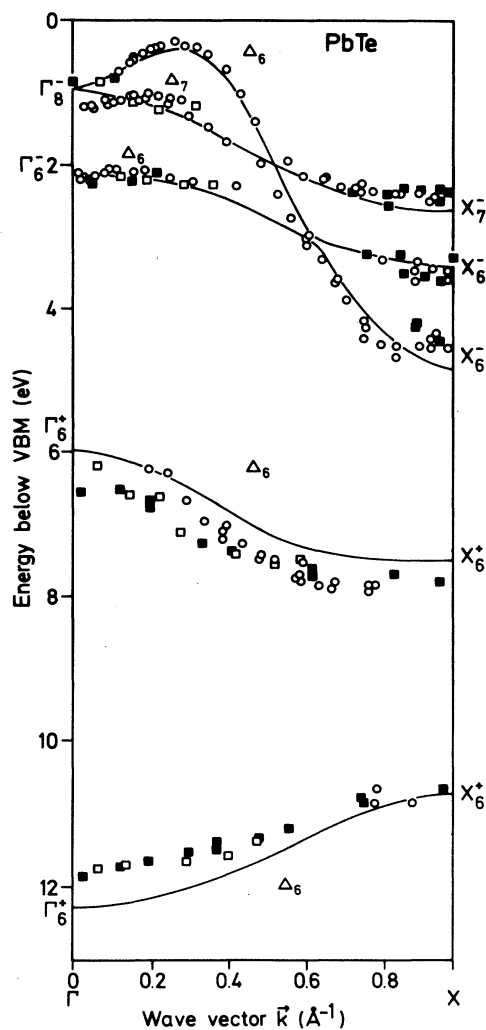


FIG. 7. Experimental band structure for PbTe, derived from spectra in Figs. 1 and 2. Transitions into the third, fourth, and fifth Brillouin zones are marked by open circles, solid squares, and open squares. The represent the results of a LMTO band-structure calculation.

TABLE II. Experimental results for the critical-point energies of PbTe along the  $\Gamma$ - $X$  line, compared with the experimental determination of Grandke *et al.* (Ref. 6) and results from several band-structure calculations.

	Experiment		Calculations			
	This work	Grandke <i>et al.</i> <sup>a</sup>	APW <sup>b</sup>	EPM <sup>c</sup>	EPM <sup>d</sup>	LMTO <sup>e</sup>
$\Gamma_8^-$	1.0	1.3	0.88	1.0	0.9	0.95
$\Gamma_6^-$	2.1	2.5	1.98	2.9	2.0	2.15
$\Gamma_6^+$	6.35			6.45	5.7	6.0
$\Gamma_6^+$	11.8			16.30	12.7	12.28
$X_7^-$	2.45	2.5	2.37	2.1	2.6	2.65
$X_6^-$	3.55	3.4	3.06	2.8	3.2	3.45
$X_6^-$	4.5	4.5(4.7)	4.63	4.20	4.5	4.85
$X_6^+$	7.85			6.35	7.4	7.5
$X_6^+$	10.75			16.15	11.3	10.7
spin-orbit splitting at $\Gamma$	1.10	1.15	1.03	1.1	1.1	1.2
spin-orbit splitting at $X$	1.10	0.9	0.67	0.7	0.55	1.35
$\Delta_6(\text{max})$	0.30	0.7	0.33	0.60	0.25	0.40

<sup>a</sup>Reference 6.

<sup>b</sup>In Ref. 6.

<sup>c</sup>Reference 14.

<sup>d</sup>Reference 13.

<sup>e</sup>This work.

what larger (but in absolute terms still small) discrepancy on the order of 0.1–0.2 eV. Note that the other band-structure calculations also give reasonable values for the spin-orbit splitting.

It is instructive to compare our experimental results and their interpretation with the photoemission data of Grandke *et al.*<sup>6</sup> These workers used rare-gas resonance lines of 16.85 and 21.22 eV photon energy, and considered dispersion effects both as a function of photon energies, as well as a function of  $\mathbf{k}$  by collecting data at different polar angles of electron emission, in the two mirror planes normal to the (100) surface. On the basis of their band-structure calculations, which included a description of the complex conduction band structure (although not within the full LEED formalism), they conclude that spectra recorded in off-normal geometries are dominated by indirect transitions in which  $\mathbf{k}$  is not conserved, while in normal emission, direct transitions play a more important role, because the number of final bands which couple strongly to the plane-wave states in the vacuum are quite small in this particular geometry. Some of these final states bear a close resemblance to a parabolic final state, such as that employed in the present study (cf. Fig. 9 of Ref. 6). As a result of their calculations, they conclude that the main contribution to the normal-emission spectra from the lead chalcogenides is due to only one conduction band. As is evident from Figs. 12 and 13 in Ref. 6, this final state is parabolic. Grandke *et al.* fit this band by a parabola with an effective-mass parameter  $\alpha=1.1$  in Eq. (1), i.e., a small deviation from the free-electron shape. Since they obtain this fit of the calculated bands between 15 and 25 eV, we believe that

there is no real discrepancy with respect to our assumption of  $\alpha=1$ , derived over a much larger range of final energies directly from experimental data (viz., the structure plot in Fig. 5). Thus there is no discrepancy between the conclusion drawn by Grandke *et al.* that the best description of the photoemission spectra is a “weighted-indirect-transition model” and our determination of the band structure of PbSe and PbTe on the basis of direct transitions. Both processes play a significant role, as can be read off directly from the spectra, from the stationary and dispersing contributions to the peak at about 6-eV binding energy in Figs. 2 and 4.

One might argue that at very low photon energies the approximation of the final state by a parabola must break down eventually. Middelmann *et al.*,<sup>19</sup> in a photoemission band-structure determination of  $\alpha$ -Sn, have indeed shown that strong deviations from parabolic behavior may occur for low final energies, and can be determined once the shape of the occupied bands is known from direct transitions at much higher photon energies. The present band-structure data were derived from transitions to three or, in the case of PbSe, even four Brillouin zones, and data from these transitions show good agreement among each other. Thus the deviation of the final band from parabolic shape is probably restricted to very low photon energies such that our band determination is now affected. Middelmann *et al.*<sup>19</sup> have shown that, in the case of  $\alpha$ -Sn, the deviations from parabolic shape were very small beyond a final energy of about 13 eV. If a similar value were to apply in the case of PbSe and PbTe, most of the data points in Figs. 6 and 7 would not be affected.

## ACKNOWLEDGMENTS

This work was supported by the Bundesministerium für Forschung und Technologie under Grant No. 05-

241-HR, as well as through the Deutsche Forschungsgemeinschaft through Sonderforschungsbereich No. 6. We thank the staff of BESSY for their support.

\*Permanent address: Istituto di Fisica, Università di Modena, Via Campi 213/a, I-41100 Modena, Italy.

†Present address: Laboratorio TASC, Padriciano 99, I-34100 Trieste, Italy.

<sup>1</sup>E. W. Plummer and W. Eberhardt, *Adv. Chem. Phys.* **49**, 533 (1982), and references therein.

<sup>2</sup>F. J. Himpsel, *Appl. Opt.* **19**, 3964 (1980); *Adv. Phys.* **53**, 1 (1983).

<sup>3</sup>T.-C. Chiang, M. Aono, F. J. Himpsel, and D. E. Eastman, *Phys. Rev. B* **21**, 3513 (1980).

<sup>4</sup>F. Solal, G. Jezequel, F. Houzay, A. Barski, and R. Pinchaux, *Solid State Commun.* **52**, 37 (1984).

<sup>5</sup>L. Sorba, V. Hinkel, H.-U. Middelmann, and K. Horn, *Phys. Rev. B* **36**, 8075 (1987).

<sup>6</sup>Th. Grandke, L. Ley, and M. Cardona, *Phys. Rev. B* **18**, 3847 (1978).

<sup>7</sup>O. K. Andersen, *Phys. Rev. B* **12**, 3060 (1975).

<sup>8</sup>N. E. Christensen, *Int. J. Quantum Chem.* **25**, 233 (1984), and unpublished. See also C. Godreche, *J. Magn. Magn. Mater.*

**29**, 262 (1982), and references therein.

<sup>9</sup>W. Braun and G. Jäkisch, *Ann. Isr. Phys. Soc.* **6**, 30 (1983).

<sup>10</sup>U. von Barth and L. Hedin, *J. Phys. C* **5**, 1629 (1972).

<sup>11</sup>G. B. Bachelet and N. E. Christensen, *Phys. Rev. B* **31**, 879 (1985).

<sup>12</sup>M. Wohlecke, A. Baalman, and M. Neumann, *Solid State Commun.* **49**, 217 (1984).

<sup>13</sup>G. Martinez, M. Schlüter, and M. L. Cohen, *Phys. Rev. B* **11**, 651 (1975).

<sup>14</sup>Y. W. Tung and M. L. Cohen, *Phys. Rev.* **180**, 823 (1969).

<sup>15</sup>W. B. Jackson and J. W. Allen, *Phys. Rev. B* **37**, 4618 (1988).

<sup>16</sup>I. W. Lyo and E. W. Plummer, *Phys. Rev. Lett.* **60**, 1558 (1988).

<sup>17</sup>F. Herman and S. Skillman, *Atomic Structure Calculations* (Prentice-Hall, Englewood Cliffs, 1963).

<sup>18</sup>S. E. Kohn, P. Y. Yu, Y. Petroff, Y. R. Shen, Y. Tsang, and M. L. Cohen, *Phys. Rev. B* **8**, 1477 (1973).

<sup>19</sup>H.-U. Middelmann, L. Sorba, V. Hinkel, and K. Horn, *Phys. Rev. B* **35**, 718 (1987).